②

AD-A208 893

DOCUMENTATION PAGE

1a. REP NC	1b. RESTRICTIVE MARKINGS NONE
2a. SEC NC	3. DISTRIBUTION / AVAILABILITY OF REPORT
2b. DEC_____CHEDULE NONE	UNLIMITED

4. PERFORMING ORGANIZATION REPORT NUMBER	5. MONITORING ORGANIZATION REPORT NUMBER(S)
Technical Report #15	

6a. NAME OF PERFORMING ORGANIZATION Stanford University	6b. OFFICE SYMBOL (If applicable)	7a. NAME OF MONITORING ORGANIZATION Office of Naval Research

6c. ADDRESS (City, State, and ZIP Code) Department of Chemical Engineering Stanford University Stanford, CA 94305-5025	7b. ADDRESS (City, State, and ZIP Code) 800 North Quincy Avenue Arlington, VA 22217

8a. NAME OF FUNDING / SPONSORING ORGANIZATION Office of Naval Research	8b. OFFICE SYMBOL (If applicable)	9. PROCUREMENT INSTRUMENT IDENTIFICATION NUMBER N00014-87-K-0426

| 8c. ADDRESS (City, State, and ZIP Code) 800 North Quincy Avenue Arlington, VA 22217-5000 | 10. SOURCE OF FUNDING NUMBERS |

PROGRAM ELEMENT NO.	PROJECT NO.	TASK NO.	WORK UNIT ACCESSION NO.

11. TITLE (Include Security Classification)

Infrared and Fluorescence Spectroscopic Studies of Self-Assembled n-Alkanoic Acid Monolayers

12. PERSONAL AUTHOR(S)
S.H. Chen and C.W. Frank

13a. TYPE OF REPORT Technical Report	13b. TIME COVERED FROM 88/6/1 TO 89/5/31	14. DATE OF REPORT (Year, Month, Day) 89/5/30	15. PAGE COUNT 19

16. SUPPLEMENTARY NOTATION

Galley proofs for Langmuir publication

17.	COSATI CODES		18. SUBJECT TERMS (Continue on reverse if necessary and identify by block number)
FIELD	GROUP	SUB-GROUP	

19. ABSTRACT (Continue on reverse if necessary and identify by block number)

Infrared and fluorescence spectroscopic methods were used to study the kinetics and thermodynamics of the formation of self-assembled films of n-alkanoic acids by adsorption from solutions. The adsorption of stearic acid from hexadecane solutions onto glass and aluminum substrates was shown to lead to monolayer formation. A Langmuir-type transient adsorption model was shown to be applicable to these systems. The stationary fluorescence spectroscopy of a pyrene-labeled alkanoic acid probe was also used to determine the relative values of the kinetic constants of various fatty acids having different number of carbons in the chains. A linear increase of approximately 230 cal/mole in the negative free energy of adsorption with increasing chain length of the fatty acids was found. This is attributed to the energetic contribution of the molecular organization of the aliphatic chains to the self-assembly process.

20. DISTRIBUTION / AVAILABILITY OF ABSTRACT ☒ UNCLASSIFIED/UNLIMITED ☐ SAME AS RPT. ☐ DTIC USERS	21. ABSTRACT SECURITY CLASSIFICATION Unclassified
22a. NAME OF RESPONSIBLE INDIVIDUAL Dr. Kenneth J. Wynne	22b. TELEPHONE (Include Area Code) (202)696-4410	22c. OFFICE SYMBOL

DD FORM 1473, 84 MAR   83 APR edition may be used until exhausted.
All other editions are obsolete.

89 6 05 097

Infrared and Fluorescence Spectroscopic Studies of Self-Assembled
n-Alkanoic Acid Monolayers

by

S. H. Chen and C. W. Frank

Prepared for Publication in Langmuir

Stanford University
Departments of Chemical Engineering and Electrical Engineering
Stanford, CA 94305

May 30, 1989

Infrared and Fluorescence Spectroscopic Studies of Self-Assembled *n*-Alkanoic Acid Monolayers

Shaun H. Chen and Curtis W. Frank*

Department of Chemical Engineering, Stanford University, Stanford, California 94305-5025

1. Introduction

Organized organic molecular monolayers formed by spontaneous adsorption from solution, known as self-assembled films, have been the subject of a number of studies reported in recent years.[1-7] As an increasing number of improved physical measurements have been used to study the self-assembled films, more and more experimental evidence has accumulated in support of the formation of these compact, well-organized which closely resemble ← *structures* Langmuir-Blodgett monolayers.[3,4] The potential, but yet to be demonstrated, application of this technique in various technologies has made it even more promising.

Amphiphilic molecules are known to form ordered molecular structures. The head/tail group interaction with the substrate is the major factor affecting film deposition in the Langmuir-Blodgett transfer process.[8,9] In the adsorption of surfactants on solid surfaces, this factor also plays an important role. In the following, we indicate several possible situations in which adsorption of surfactants occurs from solutions:

(a) Surfactants solvated in hydrophilic, polar solvents or in the form of micelles above the critical micelle concentration adsorb onto a hydrophobic adsorbent such that the hydrophobic tails of the surfactant molecules attach to the surface. The molecules line up with one another to form a monolayer, leaving the hydrophilic head groups at the surface exposed to the hydrophilic solvent.[10-12]

(b) Surfactants in hydrophilic, polar solvents adsorb onto a hydrophilic adsorbent in two steps. At first, surfactant molecules adsorb to form a layer with the hydrophilic head groups anchored to the surface and the tails lined up with one another. On top of this first layer, a second layer of surfactant molecules can then adsorb with the tails down to form a hemimicelle or bilayer structure.[10-12]

(c) Surfactants in hydrophobic, nonpolar solvents adsorb onto a hydrophilic polar surface such that the hydrophilic head groups are bound to the surface while the hydrophobic tails line up with one another, forming a monolayer.[3-6]

In all systems, the van der Waals interaction among the hydrophobic aliphatic portions of the adsorbate molecules contributes to their alignment. The tendency of these molecules to form organized monolayers increases with increasing length of the aliphatic chain.[4,9] Clearly, both the substrate-head group binding and the van der Waals attraction among the hydrocarbon chains will control the adsorption kinetics. In general, the well-known Langmuir isotherm is applicable for monolayer adsorption,[11,12] but very little kinetic data have been reported for these types of systems.

Infrared spectroscopy, either in the transmission mode,[13] the grazing incidence reflection-absorption (GIR) mode,[3-6] or the attenuated total reflection (ATR) mode,[23] has been used for the characterization and structure determination of the self-assembled monolayers. GIR-IR is especially useful in determining the molecular orientation in the film structures because it detects only the vibrational component perpendicular to the substrate surface.[1,4] Polarized ATR-IR can also be used for orientation determination.[3,14] McKeigue and Gulari[15] have used ATR-IR to quantitatively study the adsorption of the surfactant Aerosol-OT.

Fluorescence spectroscopy of systems containing small

TXT03
PAR24

fractions of covalently bound fluorescent probes within the compound of interest can provide molecular-level information about structure (e.g., configuration and molecular association), microenvironment (e.g., polarity and viscosity), and dynamics. Useful tools include various stationary fluorescence emission peak intensity ratios, excitation energy-transfer experiments, and transient depolarization measurements. The usefulness of the fluorescence probe approach has been demonstrated for a variety of systems, e.g., micellar solutions,[16] polymer adsorption,[17] and Langmuir–Blodgett films.[18]

FNT 16. FNT 17
FNT 18

PAR27

In these two spectroscopic techniques, IR measures directly the presence and orientation of molecules while fluorescence indirectly monitors their properties. Therefore, they can be considered as complementary experimental tools. However, incorporation of the probe molecules into the system may actually disturb the structure of the host systems because of the bulkiness of the aromatic fluorophores or the aggregation of them. To minimize these problems, only the minimum amount of probe molecules should be used.

PAR30

Allara and co-workers[1,4,5] and Sagiv and co-workers,[2,3,7] in their series of extensive studies using a number of characterization techniques have demonstrated that self-assembled films of structure similar to that of the Langmuir–Blodgett films can be produced under appropriate conditions. They also showed that the kinetics of adsorption is important in the formation of these organized two-dimensional films, which very few past studies have yet focused upon.

PAR33

In this paper, we report the results of our studies of the dynamics of the self-assembling adsorption process. We used IR spectroscopy to study the thermodynamic and kinetic aspects of adsorption of fatty acids from nonpolar solutions onto polar surfaces. The variation of wettability of the substrate surfaces provides an auxiliary indication of monolayer formation. We also report the application of stationary fluorescence spectroscopy of incorporated pyrene probes in adsorbed mixed monolayer films and its use as a simple method for the determination of the relative adsorption constants. Further studies on the structural aspects of these adsorbed films using fluorescence probes are currently under way in this laboratory.

TXT06

2. Experimental Section

PAR36

1. Materials. The adsorbates consisted of the homologous series of the even n-alkanoic acids, abbreviated as C_{10} through C_{22}, which were obtained from Sigma Chemical Co. Those samples with nominal purities less than 99% were recrystallized twice from ethanol. The pyrene end-tagged palmitic (hexadecanoic) acid (Py–C_{16}) was obtained from Molecular Probes, Inc., and used as received. The solvents n-hexadecane (HD), ethanol, acetone, and toluene, also from Sigma Chemical Co., were used as received. Distilled and deionized water was used for substrate cleaning and contact angle measurements. The microscope glass slides were obtained from Becton Dickinson and Co. ("Gold Seal" brand). The ATR crystal (one-pass parallelepiped KRS-5; 45°, 50 × 10 × 3 mm) was obtained from Harrick Scientific Inc.

PAR39

2. Sample Preparation. Precleaning of the solid substrates was found to be vital to the subsequent adsorption process, with the following cleaning procedures found to yield reproducible results. The microscope glass slides were first degreased with 120 °C H_2SO_4/H_2O_2 (4:1) solution for 20 min. followed by consecutive water, ethanol, and acetone rinses, and finally dried in the nonoxidizing portion of a Bunsen burner flame for ca. 10 s. The aluminum substrates were prepared by evaporating approximately 1000 Å of ultrapure aluminum onto precleaned Si wafers. (It is well-known that an aluminum surface will develop a thin top layer of natural oxide. In this work, no attempt was made to control the surface aluminum oxide thickness after the deposition of aluminum.) The aluminum substrates could be reused after cleaned with cold 5% H_2SO_4 solution for ca. 30 s, followed by water, ethanol, and acetone rinses and finally gentle-flame drying.

PAR42

Adsorbate solutions were prepared by dissolving weighed portions of the fatty acids in HD to desired concentrations covering

TXT06
PAR42

the range from 10^{-5} to 10^{-6} M. Precleaned glass vials were used as the adsorption cells. During the initial dissolution, it was necessary to warm the liquid contents to about 50 °C. The same procedure was also used to redissolve the crystals occasionally formed during solution storage, especially for the more concentrated (~0.01 M) solutions of C_{22} and C_{26}. The preparation of the monolayer films was carried out at 22 °C. To do this, the substrates were immersed in the solutions for a predetermined period of time and then removed. A strong nitrogen gas jet was used to blow off any remaining liquid droplets on the surface or the edges of the substrates.

PAR45

Pyrene-labeled mixed monolayers were prepared by adsorption from solutions of the desired concentration of a particular fatty acid, along with a small fraction of the probe Py–C_{16}. Py–C_{16} was first dissolved in HD/toluene (1:1) by warming to about 50 °C. The mixed solutions were prepared by diluting more concentrated Py–C_{16}/(HD + toluene) solutions and mixing with a host fatty acid solution to the desired molar ratios. The final solutions were of total acid concentration of 0.005 M in solvent mixtures containing about 10% by volume of toluene in HD.

PAR48

3. Characterization. A telescope–goniometer was used to measure the static contact angles of HD and water on substrates before and after adsorption of the fatty acids. Measurements were made under atmospheric conditions. A ~~Rang-Hui~~ _Gaertner_ ellipsometer with a He–Ne laser source was used to measure the film thickness.

PAR51

Infrared spectra of the adsorbed films were obtained with a Perkin Elmer 1710 FTIR spectrometer, equipped with a DTGS detector and a nitrogen-purged sample chamber. The transmission IR spectra of the adsorbed species were directly measured on the glass slides. The ATR-IR spectra were taken on the same spectrometer, using a multiple internal reflection attachment obtained from Harrick Scientific Inc. The ATR-IR spectra of adsorbed species were obtained by pressing two film-covered substrates against the internal reflection surfaces of the ATR crystal. All spectra were taken with 4-cm^{-1} resolution. In practice, it was usually necessary to average 1000–2000 scans in order to obtain spectra of acceptable signal-to-noise ratio. The reference spectra, taken with clean substrates prior to adsorption, were _subtracted_ from the sample spectra during data processing.

PAR54

Fluorescence emission spectra of the pyrene-doped monolayers were obtained with a Spex Fluorolog 212 spectrofluorometer with a 450-W Xenon arc lamp. The excitation wavelength was set at 343 nm, and the spectra were taken in the front-face mode. Because of the low signal intensity from these monolayer samples, wide slit widths were used (2 mm), and multiple scans (two to five) were averaged.

TXT09

3. Results

PAR57

1. Surface Wettability and Monolayer Formation.

It is well-known that the change in surface wettability of the substrate can reflect the adsorption of the amphiphilic molecules.[1-6] In this work, it was used as a qualitative indicator. Clean glass and aluminum substrates were wetted by both water and hexadecane; i.e., they are both hydrophilic and oleophilic. The measured contact angles were small, approximately 5° (±4°). After the adsorption of the amphiphilic fatty acid molecules, the surface wettability was drastically altered, as indicated by the sheeting-off of the oil solutions. Contact angle measurements of equilibrated samples indicated that the fatty acid/Al films were both hydrophobic and oleophobic, as has been reported previously.[3,4] The static water contact angle on equilibrated fatty acid/Al samples obtained was about 97° (±2°), and the static hexadecane contact angle was about 47° (±2°). For fatty acid/glass samples, the hexadecane contact angle was close to that of fatty acid/Al. However, the water contact angle was small (5–10°), and the fatty acid monolayers were apparently lifted off by water,[3] as indicated by subsequent hexadecane contact angle and IR measurements.

PAR60

To confirm the formation of monolayers, the thickness of equilibrated fatty acid films C_{14}–C_{22}/Al was measured by ellipsometry. The results, which are given in Table I, are very similar to those previously reported by Allara and Nuzzo[4] and show that the film thicknesses correspond to the extended zig-zag molecular lengths of the film-forming molecules. This suggests that they are indeed monolayers,

TBL I (006, 9–10)

TXT09
PAR60

9   with the fatty acid chains organized approximately per-
16 pendicular to the substrates.

PAR63

SEN03   1   The chemical composition of the substrate has been
10 known to play a vital role in the formation of adsorbed
SEN06   21 films.[3] We have also attempted the same immersion–re-
8   moval procedure of film preparation with Si (having a thin
SEN09   18 top layer of native oxide) and quartz substrates. No
3   oleophobic films of fatty acid were formed by adsorption,
SEN12   12 consistent with that previously reported. A possible ex-
4   planation of this observation involves the metal oxide
SEN15   12 composition of the substrate. According to data from the
7   manufacturer, the glass slides used in the present work
16 contain approximately 72.6% silica, along with several
23 other metal oxides, the major ones being Na_2O (14.1%),
SEN18   32 CaO (7.1%), MgO (3.6%), and Al_2O_3 (1.8%). These metal
4   atoms present on the surface could promote the anchoring
13 of the acid head group, perhaps by chemical bonding (salt
23 formation indicated by infrared spectra), while the van der
32 Waals interaction among the aliphatic tails of the mole-
40 cules stabilizes the molecules within the adsorbed layer,
SEN21   49 perhaps by crystallization. The lack of these additional
7   metal ions in pure silica may lead to poor anchoring.

PAR66

SEN03   1   The binding strength of the fatty acid monolayers to the
12 glass substrate is lower than those to the (oxidized) alu-
21 minum substrates, as indicated by the poor resistance of
30 fatty acid/glass to water compared to the total stability
SEN06   39 of fatty acid/Al. This could also be attributed to the
9   smaller extent of metal–acid interaction in films on glass
SEN09   18 than those on aluminum. When in contact with water, the
8   adsorbed fatty acid molecules on the nonmetal (i.e., SiO_2)
17 sites of the surface may be replaced by water molecules
27 since the physical binding of the acid head group to SiO_2
38 is weaker than the site–water interaction.

PAR69

SEN03   1   2. Infrared Spectra of Adsorbed Films. Transmis-
SEN09   2   sion infrared spectra of the adsorbed species were obtained
11 for the IR transparent range of glass (wavenumber > 2500
21 cm^{-1}), which contains the CH_2 and CH_3 stretch peaks of
SEN12   31 the aliphatic tails of the fatty acid molecules. A typical
4   unpolarized transmission-IR spectrum of two stearic acid
11 monolayers (one monolayer on each side of the glass slide)
21 adsorbed from 0.01 M hexadecane solution at equilibrium
SEN15   29 is shown in Figure 1. This spectrum is similar to the
8   high-frequency portion of the bulk spectrum of stearic acid
17 obtained from a dispersion in a KBr pellet (not shown),
27 with peaks assignable to the CH_2 symmetric and asym-
35 metric stretches (2850 and 2920 cm^{-1}, respectively) and the
44 CH_3 symmetric and asymmetric stretches (2890 and 2962
52 cm^{-1}, respectively).

FIG 1 (012,33–34)

PAR72

SEN03   1   To obtain the full-range IR spectrum of the adsorbed
SEN06   11 species, unpolarized ATR measurements were made. Two
3   substrates with adsorbed films prepared in the same way
12 were pressed against the two ATR crystal surfaces so that
22 the adsorbate was sampled by the internally reflected IR
SEN09   31 beam. A moderate pressure was necessary in order to
10 "push" the substrate surface into the penetration range of
19 the IR beam, which is on the order of several thousand
SEN12   30 angstroms. After some experimentation, a suitable
7   pressing condition was determined, and reproducible
SEN15   13 spectra could be obtained. However, the detailed effect
6   of the pressure exerted by the plates on the molecular
16 organization in the fatty acid films may be rather com-
SEN18   25 plicated and will not be discussed here. Shown in parts
5   a and b of Figure 2 are the typical ATR-IR spectra of
17 adsorbed stearic acid adsorbed at equilibrium on glass and
SEN21   26 Al substrates, respectively. One significant difference
5   between spectra on these two substrates is that only the
15 1420/1470- and 1580-cm^{-1} peaks, assigned to the symme-
22 tric and asymmetric COO^- stretches, were observed for
30 C_{18}/Al, while the 1730-cm^{-1} peak, assigned to the free acid
40 C=O stretch, was seen in addition to the carboxylate
SEN24   49 stretches for C_{18}/glass. This implies that on the Al sub-
8   strate the anchoring acid head groups were totally de-
18 protonated into salt (COO^-),[4] but on the glass substrate

FIG 2 (018.10–11)

TXT09
PAR72

only a portion of them were deprotonated on adsorption, the remainder remaining as free acid. This is also consistent with the discussion of the previous section in that the metal atoms on the surface can cause deprotonation of the adsorbed acid head group and the Si portions cannot.

PAR75

3. Transient Adsorption Behavior. Unpolarized transmission-IR or ATR-IR was used to follow the variation of the peak intensities of C_{18} adsorbed films prepared for various times of immersion from solutions of various adsorbate concentrations. Contact angle measurement was used to follow the surface wettability change with time. With solutions of relatively low concentrations (10^{-2}–10^{-4} M for glass substrate and 10^{-4}–10^{-6} M for aluminum substrate), the initial variation of IR peak intensities and contact angles with the time of immersion could be observed. *Both the IR adsorption peak intensities and the contact angles increased initially with increasing time of immersion as well as increasing adsorbate concentration,* and they asymptotically reached plateau values at long immersion times and high solution concentrations. The time required to reach the maximum nonwettability increases with decreasing concentration of adsorbate solution.

PAR78

Parts a and b of Figure 3 show the 2920-cm^{-1} transmission IR peak intensity and the HD contact angle variation for C_{18}/glass, and parts c and d of Figure 3 show the 2920-cm^{-1} ATR-IR peak intensity and the water and HD contact angle variation for C_{18}/Al, respectively. The intensity of the peaks other than the 2920-cm^{-1} one also increased proportionately. The plateau intensities of the high-frequency peaks (CH$_2$ and CH$_3$ stretches) were quite reproducible, up to about ±5%, which is essentially the error of IR measurement at this intensity level. However, the reproducibility of the carbonyl and carboxylate stretch peaks in the lower frequency range was somewhat worse (±20%).

PAR81

4. Fluorescence of Monolayers Containing Pyrene-Labeled Probes. In order to utilize the fluorescence probe method to study the self-assembled films, measurements were performed on alkanoic acid monolayers containing a pyrene-labeled probe. They were prepared on the Al substrates instead of the glass slides because an impurity fluorescence of the glass slides caused difficulties in the analysis of the spectra. With fluorescence probes positioned very close to a metal surface, the fluorescence intensity is strongly quenched by the metal.[19] In this case, considering that the pyrene groups are located within 100 Å of the aluminum surface (the native oxide layer on Al was approximately 50 Å thick), the estimated pyrene fluorescence lifetime is about 1 order of magnitude less than the solution values. Nevertheless, good fluorescence spectra can still be obtained.

PAR84

Mixed monolayers containing the fluorescence probe pyrene hexadecanoic acid, Py-C_{16}, in host fatty acids of even-numbered carbons from C_{10} to C_{22} were prepared by adsorption from solutions containing mostly the host fatty acid and 1-5 mol % of Py-C_{16}. All monolayers were prepared under equilibrium adsorption conditions.

PAR87

A typical fluorescence emission spectrum of a Py-C_{16}/C_{18} mixed monolayer prepared from an HD solution of 0.005 M total acid in which 2% was Py-C_{16} is shown in Figure 4. Although the spectrum of pyrene and its derivatives has appeared in many places in the literature, we reproduce a typical spectrum here to demonstrate the quality of data obtainable for these low concentration doped monolayers. The shape of this spectrum is similar to the usual pyrene emission, with peaks between 370 and 430 nm.

PAR90

There is no significant excimer formation, as demonstrated by the lack of a peak at about 470 nm. In all cases studied here (host length ≈ 14-22 carbons; 1-5% guest in

absorption

FIG 3 (003, 8– 9)

FNT 19

FNT 20

FIG 4 (003,31–32)

TXT09
PAR90

adsorbate solution), the I_E/I_M values of the emission ranged between 0.01 and 0.05. This shows that the Py–C$_{16}$ molecules did not aggregate within the adsorbed monolayers, and thus we can assume the chromophores were randomly distributed in the mixed monolayers. It should be noted that the concentration of the probe molecules in the adsorbed monolayers may not be identical with the fraction of the probe within the total adsorbate concentration. Judging from the excimer fluorescence content, the fraction of probe in the adsorbed films is likely less than that in the adsorbate solutions.

PAR93

Since the fluorescence observed for the mixed monolayers was predominantly from isolated pyrene chromophores, the monomer emission intensity should correspond to the amount of Py–C$_{16}$ adsorbed on the substrate. With host fatty acids of carbon number greater than about 14, the pyrene monomer emission intensity was found to indeed vary with the preparation conditions. Figure 5 shows the 377-nm peak intensity of mixed monolayers prepared at equilibrium from solutions of 1–4.8% tagged acids in 0.005 M total concentration. The intensity increased approximately linearly with the molar fraction of Py–C$_{16}$ in solution and decreased by about half as the carbon number of the host fatty acid increased by 2. With host fatty acids C$_{14}$ and lower, however, this trend was not followed. For these short chains, a different adsorption mechanism may be dominant or the adsorbed film may be disordered.

TXT12

4. Discussion

SEN03

PAR96

1. Adsorption Kinetics and Transient Langmuir Kinetic Model. The IR and contact angle data, shown in Figure 3a–d, show almost identical trends, as previously discussed. The change in water and HD contact angles indicates the change in surface chemical composition of the substrates. Clean glass and aluminum surfaces have contact angles close to zero, while at long immersion times and with high enough solution concentrations the contact angles of the adsorbed films approach plateau maximum values. The parallelism of the increase in the contact angles and the IR absorbance suggests that these two measurements monitor the same quantity—the surface coverage of the adsorbate. Intermediate values of contact angles and adsorbance between the initial and the maximum values correspond to intermediate surface coverages. At these intermediate coverages, the adsorbate molecules are prehaps organized in a patchlike fashion, and the contact angle measurement, which takes a macroscopic average over a certain surface area, picks up some "average" value between that of the clean surface and the fully covered one.

PAR99

If we assume that the plateau adsorption at the highest solution concentrations corresponds to the full coverage of the surface "sites" of the substrate, as for the monolayer adsorption, the fractional coverages of the substrate surface can then be calculated from the normalized IR peak intensities. From theoretical considerations, monolayer adsorption can be thought of as a surface site filling procedure, with the adsorption and desorption steps counteracting each other.

PAR102

Here, we also neglect the diffusional mass-transfer resistance, as has previously been validated by Grow and Shaeiwitz[21] for adsorption of several surfactants from aqueous solutions. In general, for the adsorption of surfactants onto planar surfaces, the surface concentration of the adsorbate is so small that the adsorption step is always rate-controlling. In this manner,[21-23] a transient Langmuir adsorption kinetic model can be written as

$$\frac{d\theta}{dt} = \frac{k_a}{N_0}c(1 - \theta) - \frac{k_d}{N_0}\theta \qquad (1)$$

where θ is the fractional surface coverage calculated from the normalized IR peak intensity, t is the adsorption time, k_a and k_d are the adsorption and desorption rate constants,

FIG 5 (009, 3- 4)

absorbance

FNT 21-23

REQU 1 (009.14-15)

TXT12
PAR102

N_0 is the surface adsorbate concentration at full coverage, and c is the solution concentration of adsorbate.

PAR105

SEN03 Integration with the initial condition $\theta = 0$ at $t = 0$ gives

$$\theta = \frac{k_a c}{k_a c + k_d}\left(1 - \exp\left[-\frac{k_a}{N_0}\left(c + \frac{k_d}{k_a}\right)t\right]\right) \quad (2)$$

SEN06 This equation reduces to the Langmuir adsorption iso-
therm at equilibrium, i.e., as $t \to \infty$

$$\theta_{eq} = \frac{k_a c}{k_a c + k_d} = \frac{c}{c + \kappa} \quad (3)$$

where

$$\kappa \equiv k_d/k_a \propto \exp(\Delta G_a^\circ/RT)$$

and ΔG_a° is the free energy of adsorption at infinite dilution.

PAR108

SEN03 For the adsorption of C_{18} from solutions of concentrations between 10^{-2} and 10^{-6} M onto glass slides, the transient absorbance data obtained in section 3.3. can be used for kinetic calculations. Figure 6a shows the transient surface coverage obtained by normalizing the 2920-cm^{-1} IR absorption peak intensities, such as those shown in Figure 3a, to the plateau value at higher solution concentrations ($c \geq 5 \times 10^{-3}$ M) and long enough immersion times ($t \geq 5$ min). For solutions of concentration on the order of 10^{-2} M, full coverage ($\theta = 1$) was reached in a couple of minutes. On the other hand, for very dilute solutions, it took hours to reach the equilibrium coverages, θ_{eq}, which were less than unity. The equilibrated coverage data, obtained with glass slides immersed in solutions for 24 h, were also reasonably well fitted with eq 3, as shown in Figure 6b. Using the value of κ obtained, we used the functional form of eq 2 to fit the data (as shown by the curves in Figure 6a) with an exponential constant, which should equal $(-k_a/N_0)(c + k_d/k_a)$. As a check for fitting, the exponential constants obtained were plotted against c, as shown in Figure 6c. As can be seen, the fitting of the model was reasonably good.

PAR111

SEN03 From the above data fitting, the numerical value $\kappa = (1.5 \pm 0.1) \times 10^{-6}$ mol/cm^3 was obtained, which in turn gives the free energy of adsorption $\Delta G_a^\circ = -7.3 \pm 0.1$ Kcal/mol for C_{18}/glass. The numerical values of the adsorption and desorption rate constants k_a and k_d can be obtained from the fitting, if the surface concentration at full coverage, N_0, is known. If we assume $N_0 = 8.3 \times 10^{-10}$ mol/cm^2, which corresponds to an area of ≈ 20 Å^2 per fatty acid molecule (the area projected in the transverse direction taken up by a closely packed carbon chain),[9] we find that $k_a = (1.0 \pm 0.1) \times 10^{-6}$ cm/s and $k_d = (1.5 \pm 0.1) \times 10^{-14}$ mol/(cm^2·s).

PAR114

SEN03 Parts a and b of Figure 7 show similar results for the adsorption of stearic acid from solutions of concentrations between 10^{-4} and 10^{-6} M onto aluminum substrates, again obtained by monitoring the normalized 2920-cm^{-1} ATR-IR absorption peak intensity. The trends observed in this system are the same as those of the C_{18}/glass case, but the range of solution concentration over which significant coverage variation can be seen is quite different. For solution concentrations greater than about 0.001 M, the adsorption was very rapid, much faster than in the C_{18}/glass case. Again, the fits were reasonably good, and we obtain $\kappa = (5.0 \pm 0.4) \times 10^{-10}$ mol/cm^3 and $\Delta G_a^\circ = -9.2 \pm 0.1$ kcal/mol for C_{18}/aluminum. If we again assume $N_0 = 8.3 \times 10^{-10}$ mol/cm^2, we estimated that $k_a = (5.2 \pm 0.4) \times 10^{-4}$ cm/s and $k_d = (2.6 \pm 0.3) \times 10^{-11}$ mol/(cm^2·s).

PAR117

SEN03 These kinetic constants may be underestimations because the actual N_0 may be greater than the ideal value as a result of surface roughness.[7] In this work, no attempt was made to control the surface roughness of either type of substrate. The glass slides received from the manufacturer were not microscopically smooth, and the ther-

TXT12
PAR117

mally grown aluminum oxide on the evaporated aluminum substrate will also lead to a considerable degree of surface roughness.

PAR120

The adsorption and desorption constants k_a and k_d can be mathematically described by a one-dimensional interaction energy profile model.[20,21] This is illustrated schematically in Figure 8, where φ is the adsorbate–surface interaction energy and x is the distance between the adsorbate and the surface. On the basis of an order-of-magnitude analysis assuming a square-well-type profile, Grow and Shaeiwitz[21] determined k_a as a function of the adsorption barrier φ_{max} and k_d as a function of the desorption barrier ($\varphi_{max} - \varphi_{min}$). According to their calculations, the k_a and k_d values obtained in this study correspond to adsorption and desorption barriers on the order of $12kT$ and $28kT$, respectively, for C_{18}/Al and $18kT$ and $31kT$, respectively, for C_{18}/glass. The φ_{max} value of C_{18}/Al is smaller than that of C_{18}/glass, but the $-\varphi_{min}$ value of C_{18}/Al is greater than that of C_{18}/glass. The high adsorption barrier, φ_{max}, is mostly from the negative entropy of adsorption due to the loss of configurations of the hydrocarbon chains.[20] However, the φ_{max} values obtained here show that there is still a difference due to the substrate, perhaps not only resulting from the adsorbate–surface interaction but also the difference in surface roughness.

PAR123

For adsorption of surfactants from aqueous solutions on polar surfaces, although the mechanism is bilayer formation, the Langmuir kinetics has been applied to the adsorption of the first monolayer. Tabulated in Table II is an order-of-magnitude comparison of our results with the kinetic constants reported for adsorption of a number of surfactants from solutions obtained by using the Langmuir-type model.

PAR126

A detailed comparison between different systems is not possible because of factors such as the pore diffusion mass transfer resistance for particulate adsorbents, the effect of different adsorbents, the preparation or cleaning conditions, and the ionic strength effect for aqueous solutions. However, the comparison shows that the parameters k_a, k_d, and κ obtained for stearic acid → glass in this work were roughly of the same order of magnitude as those obtained in most other studies for surfactants of comparable chain length adsorbed onto glass, alumina, or similar adsorbents. The two cases that showed the most discrepancy were as follows: (1) κ and k_d were notably high for the cetylpyridinium chloride → TiO_2 system,[23] in which there is possibly a different head group orientation; (2) k_a was particularly low for the Aerosol-OT → Ge system,[15] in which the surfactant has rather short chains and the adsorbent Ge is a rather inactive substance. The most significant observation of these results is that the values of $1/\kappa$ and k_a for stearic acid → Al are significantly greater than those for any other system with particulate mineral adsorbent studied. This indicates that the adsorbing ability of metallic aluminum (even oxidized) is considerably higher relative to the mineral oxides.

PAR129

For practical purposes, the adsorption kinetic model can be used to calculate the necessary concentration and time of immersion needed to prepare a compact monolayer on a particular solid substrate surface. The dependence of κ on the hydrocarbon chain length will be discussed in the next section.

PAR132

2. Determination of Relative Adsorption Constants. If we use a Langmuir-type, two-component, competitive adsorption model, the fractional coverage of the guest molecule, θ_g, can be expressed as

$$\theta_g = \frac{c_g/\kappa_g}{c_g/\kappa_g + c_h/\kappa_h + 1} \propto I \qquad (4)$$

where κ_g and κ_h are the equilibrium constants, as defined in eq 3, for the guest molecule Py–C_{16} and the host fatty acid, respectively. I is the monomer fluorescence (377 nm)

FIG 8 (006, 8– 9)

TBL II (006, 5– 6)

REQU 4 (009,22–23)

TXT12
PAR132
SEN16 9 *intensity. Under the experimental conditions used, $c_g \ll$*
       9 c_h, $\theta_h \sim 1$, and eq 4 reduces to*

$$\theta_{g/h} = \frac{c_g}{c_g + \kappa_g/\kappa_h} \tag{5}$$

PAR135
SEN03   1   The constant κ_g for the guest molecule is unknown,
       11 leading to unknown probe concentration in the films, as
SEN06 20 mentioned in section 3.4. However, this problem can be
        7 eliminated by taking the ratio of the slopes of any two lines
       19 in Figure 5, which equals the ratio of the constants κ_h
       30 between host fatty acids (such as $\kappa_h(C_{22})/\kappa_h(C_{20})$, κ_h-
SEN09 37 $(C_{20})/\kappa_h(C_{18})$, etc.). These ratios, in turn, give the difference
        9 of the free energy of adsorption between various host fatty
SEN12 19 acids. With the value for C_{18}/Al obtained in section 4.1.
       11 as the starting point, the $-\Delta G_a^\circ$ values for other fatty acids
       22 can then be calculated, as shown in Figure 9.

PAR138
SEN03   1   As previously discussed, the Langmuir adsorption model
        9 does not apply for systems with fatty acids shorter than
SEN06 19 C_{12}. It is possible that for these systems there is a different
       13 and complicated adsorption mechanism, such as multilayer
       20 formation, as Allara and Nuzzo have suggested on the basis
       30 of their ellipsometry measurements.[4]
PAR141
SEN03   1   For fatty acids long enough to achieve the Langmuir
       11 adsorption behavior, based on the energy additivity, the
       19 contribution made by the head group, $-\Delta G_a^{\circ,h}$, and that
       28 of the N_c methylene groups to the free energy of adsorption
       39 of a surfactant may be separated as

$$-\Delta G_a^\circ = -\Delta G_a^{\circ,h} + N_c W \tag{6}$$

       46 where W is the energetic contribution of the carbon chain
SEN06 56 per unit methylene group. As shown in Figure 9, there is
        9 a linear increase in the negative free energy of adsorption,
       19 and from eq 2 we obtained $W = 230 \pm 20$ cal/mol per CH_2
SEN09 33 in the aliphatic tail. This can be interpreted as the con-
        8 tribution of the van der Waals interaction among the al-
       17 iphatic chains to the stabilization of the adsorbed am-
       25 phiphilic molecules.
PAR144
SEN03   1   Bigelow, Glass, and Zisman[24] used a temperature of
       10 wetting method to obtain the energy of adsorption of a
SEN06 20 series of amphiphiles on platinum. They also observed an
        6 increase in the (negative) energy of adsorption with in-
SEN09 14 creasing hydrocarbon chain length. In several other studies
        6 on the adsorption of surfactants to air/water or oil/water
       15 interfaces, such a trend has also been observed, but usually
SEN12 25 with a higher value of W. A comparison of these experi-
        6 mental values is given in Table III.

PAR147
SEN03   1   It can be noted that except for one drastically different
       12 result ($W = 1200$ cal/mol for alkanoic acids/oil $\rightarrow$ Pt), the
       23 W values obtained for various surfactants adsorbed onto
       31 metal surfaces from either oil solutions or melt generally
SEN06 40 fell in the range 200-400 cal/mol. This is quite reasonable
        6 since the melt of the surfactants has, in principle, very
       16 similar properties to the hydrocarbon (e.g., HD) solutions.
SEN09   1 For surfactants/water $\rightarrow$ water interface systems, the value
       10 of W fell in the range 700-800 cal/mol, significantly higher
SEN12 20 than that for oil, melt, or vapor systems. This is perhaps
        5 due to the strong repulsion of water against the aliphatic
       15 chains.
PAR150
SEN03   1   The trend of a linear increase in $-\Delta G_a^\circ$ with N_c also
       13 explains the inability of shorter fatty acids (e.g., $N_c < 10$)
SEN06 24 to self-assemble. As N_c decreases, the energy of adsorption
        9 decreases correspondingly, and at some point either the
       17 required concentration becomes greater than the available
       24 solubility or the rate of adsorption becomes too slow for
       34 any detectable adsorption to occur.
TXT15
SEN03   1   **5. Summary**
PAR153
SEN03   1   In summary, we have presented results of infrared and
       11 fluorescence studies of the kinetics and thermodynamics
       18 of the self-assembly of fatty acid on planar solid substrates
SEN06 28 from oil solutions. We obtained the Langmuir-type rate

TXT15
PAR153
7 constants of adsorption (related to the mechanism of ad-
15 sorption) and the variation of the free energy of adsorption
SEN09 25 (related to the thermodynamics of adsorption). These
3 results can indeed help shed light on the understanding
SEN12 12 of this type of systems. For further understanding of the
7 self-assembly process, detailed studies on such important
14 aspects as the substrate–adsorbate interaction and the
21 effect of surface roughness remain to be done.
TXT18
PAR156

FNN02
FNP03
SEN03 1   (1) Troughton, E. B.; Bain, C. D.; Whitesides, G. M.; Nuzzo, R. G.;
SEN06 14 Allara, D. L.; Porter, M. D. *Langmuir* 1988, 4, 365. Strong, L.; Whitesides,
5 G. M. *Langmuir* 1988, 4, 546.
FNN03
FNP06
SEN03 1   (2) Maoz, R.; Sagiv, J. *Langmuir* 1987, 3, 1034.
FNN04
FNP09
SEN03 1   (3) Maoz, R.; Sagiv, J. J. *Colloid Interface Sci.* 1984, 100, 465. Gun,
SEN09 3 J., Iscovici, R.; Sagiv, J. J. *Colloid Interface Sci.* 1984, 101, 201. Gun, J.;
4 Sagiv, J. J. *Colloid Interface Sci.* 1986, 112, 457.
FNN05
FNP12
SEN03 1   (4) Allara, D. L.; Nuzzo, R. G. *Langmuir* 1985, 1, 45; 1985, 1, 52.
FNN06
FNP15
SEN03 1   (5) Nuzzo, R. G.; Fusco, F. A.; Allara, D. L. *J. Am. Chem. Soc.* 1987,
16 109, 2358.
FNN07
FNP18
SEN03 1   (6) Boerio, F. J.; Chen, S. L. *J. Colloid Interface Sci.* 1980, 73, 176.
FNN08
FNP21
SEN03 1   (7) Sagiv, J. *J. Am. Chem. Soc.* 1980, 102, 92; *Isr. J. Chem.* 1979, 18,
16 339; 1979, 18, 346.
FNN09
FNP24
SEN03 1   (8) Roberts, G. G. *Adv. Phys.* 1985, 34, 475.
FNN10
FNP27
SEN03 1   (9) Gaines, G. L. *Insoluble Monolayers at Liquid–Gas Interfaces*;
10 Interscience: New York, 1966.
FNN11
FNP30
SEN03 1   (10) Rosen, M. J. *Surfactants And Interfacial Phenomena*; Wiley:
11 New York, 1978.
FNN12
FNP33
SEN03 1   (11) Tadros, Th. F., Ed. *Surfactants*; Academic Press: New York,
12 1984.
FNN13
FNP36
SEN03 1   (12) Kitchener, J. A. *J. Photogr. Sci.* 1965, 13, 152.
FNN14
FNP39
SEN03 1   (13) Hasegawa, M.; Low, M. J. D. *J. Colloid Interface Sci.* 1969, 29,
14 593; 1969, 30, 378.
FNN15
FNP42
SEN03 1   (14) Yang, R. T.; Low, M. J. D.; Haller, G. L.; Fenn, J. *J. Colloid
SEN06 16 Interface Sci.* 1973, 44, 249. Haller, G. L.; Rice, R. W. *J. Phys. Chem.*
11 1970, 74, 4386.
FNN16
FNP45
SEN03 1   (15) McKeigue, K.; Gulari, E. In *Surfactants in Solution*; Mittal, K.
12 L., Lindman, B., Eds.; 1984; Vol. 2, p 1271.
FNN17
FNP48
SEN03 1   (16) Turro, N. J.; Barretz, B. I.; Kuo, P. L. *Macromolecules* 1984, 17,
SEN06 14 1321. Chandar, P.; Somasundaran, P.; Turro, N. J. *Macromolecules* 1988,
11 21, 950.
FNN18
FNP51
SEN03 1   (17) Chandar, P.; Somasundaran, P.; Turro, N. J.; Waterman, K. C.
SEN06 12 *Langmuir* 1987, 3, 298. Avnir, D.; Busse, R.; Ottolenghi, M.; Wellner, E.;
10 Zachariasse, K. A. *J. Phys. Chem.* 1985, 89, 3521.
FNN19
FNP54
SEN03 1   (18) Murakata, T.; Miyashita, T.; Matsuda, M. *Langmuir* 1986, 2, 786.
SEN06 1 Tamai, N.; Yamazaki, T.; Yamazaki, I. *J. Phys. Chem.* 1987, 91, 841.
SEN09 1 Tamai, N.; Yamazaki, T.; Yamazaki, I. *J. Phys. Chem.* 1987, 91, 3572.
FNN20
FNP57
SEN03 1   (19) Waldeck, D. H.; Alivisatos, A. P.; Harris, C. B. *Surf. Sci.* 1985,
SEN06 14 158, 103. Chance, R. R.; Prock, A.; Silbey, R. In *Adv. Chem. Phys.* Rice,
14 S. A., Prigogine, I., Eds.; 1978; Vol. 37, p 1.
FNN21
FNP60
SEN03 1   (20) Prieve, D. C.; Ruckenstein, E. *AIChE J.* 1976, 22, 276.
FNN22
FNP63
SEN03 1   (21) Grow, D. T.; Shaeiwitz, J. A. *J. Colloid Interface Sci.* 1982, 86,
14 239.
FNN23
FNP66

FNN23
FNP66
SEN03   1   (22) Trogus, F. J.; Sophany, T.; Wade, W. H. *Soc. Pet. Eng. J.* 1977,
        15   *17*, 337.
FNN24
FNP69
SEN03   1   (23) Dobiás, B. *Colloid Polym. Sci.* 1978, *256*, 465.
FNN25
FNP72
SEN03   1   (24) Bigelow, W. C.; Glass, E.; Zisman, W. A. *J. Colloid Sci.* 1946, *2*,
        15   563.
FNN26
FNP75
SEN03   1   (25) Smith, R.; Tanford, C. *Proc. Natl. Acad. Sci. U.S.A.* 1973, *70*, 289.
FNN27
FNP78
SEN03   1   (26) Posner, A. M.; Anderson, J. R.; Alexander, A. E. *J. Colloid Sci.*
        14   1952, *7*, 623.
FNN28
FNP81
SEN03   1   (27) Ward, A. F. H.; Tordai, L. *Trans. Faraday Soc.* 1946, *42*, 413.
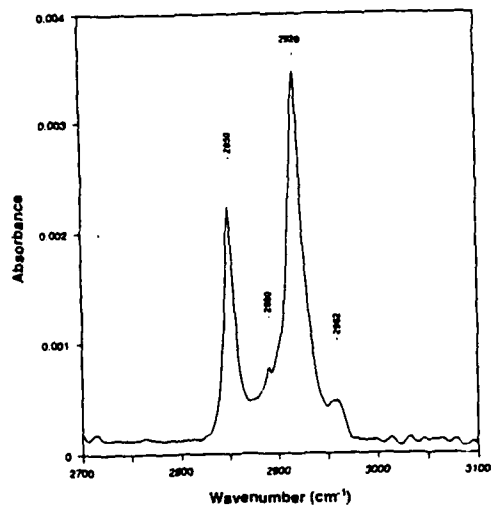
FNN28
FNP81

CAP00 1   Figure 1. High-frequency-range transmission IR spectrum of
CAP03 7   two stearic acid (C$_{18}$) monolayers (one monolayer on each side)
       17 adsorbed on a glass slide from 0.01 M solution in HD; immersion
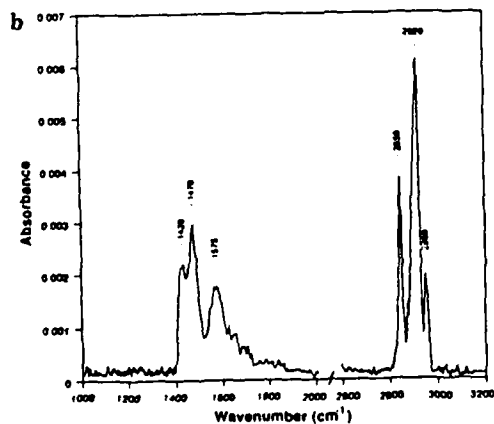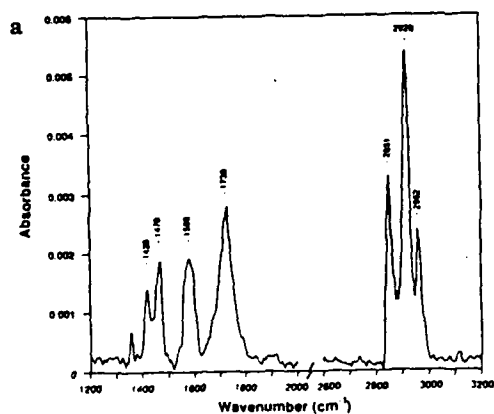   29 time = 30 min.

CAP00 1   Figure 2. Unpolarized ATR-IR spectrum of one stearic acid (C$_{18}$)
CAP03 10 monolayer adsorbed on a (a) glass slide and (b) evaporated alu-
       20 minum substrate (with an oxide layer on top) from 0.01 M solution
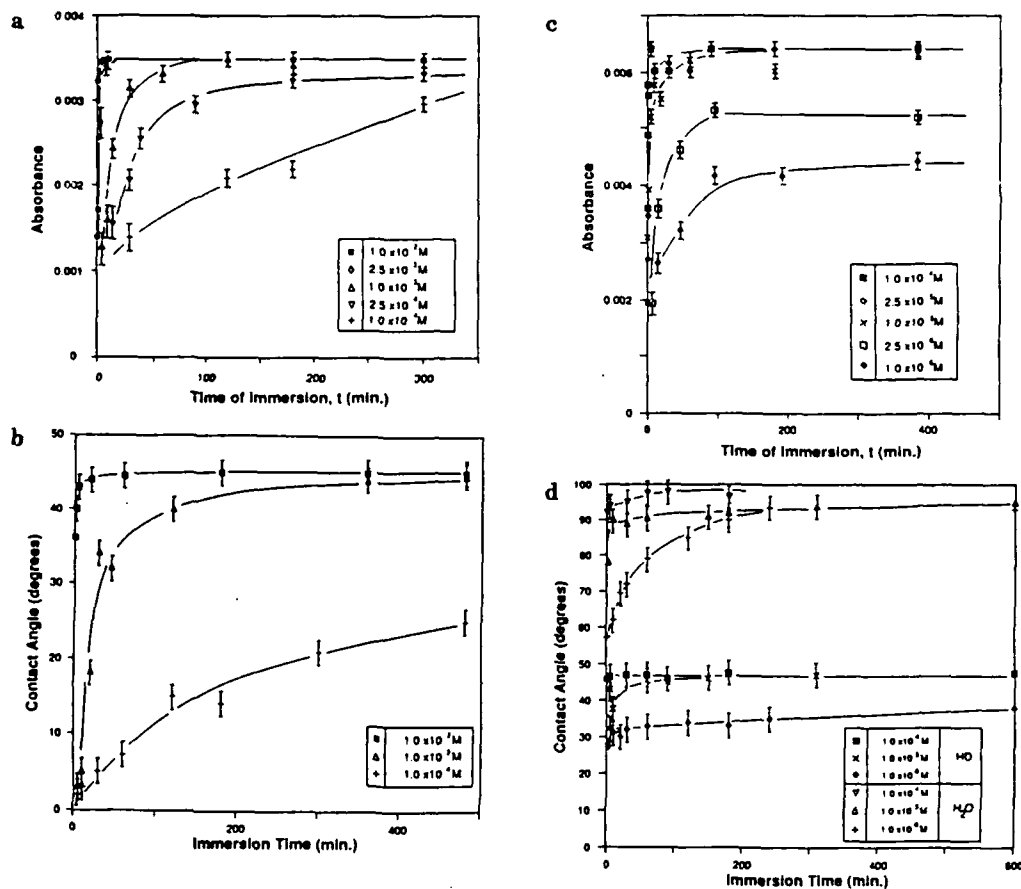   32 in HD; immersion time = 30 min.

FNN28
FNP81

Figure 3. Transient adsorption behavior of C_{18} from HD solutions monitored by infrared spectroscopy and contact angle: (a) glass slides, 2920-cm^{-1} transmission IR peak intensity; (b) glass slides, HD contact angle; (c) aluminum substrates, 2920-cm^{-1} peak intensity; (d) aluminum substrates, H_2O and HD contact angles.
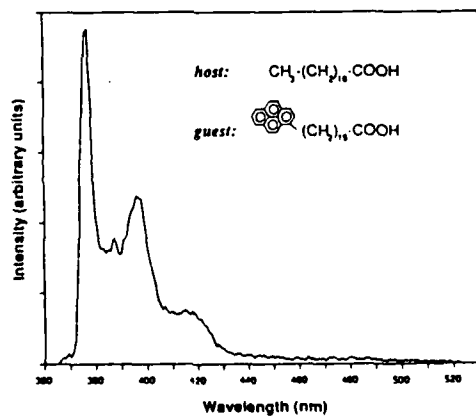
Figure 4. Typical fluorescence emission spectrum of Py–C_{16}/C_{18} mixed monolayer adsorbed on aluminum substrate from solution of 0.005 M total acid concentration containing 2% Py–C_{16} by mole.
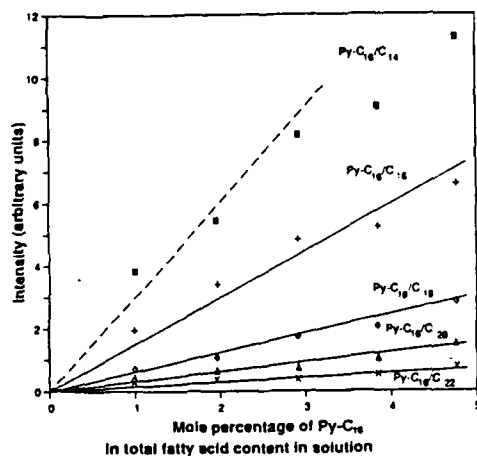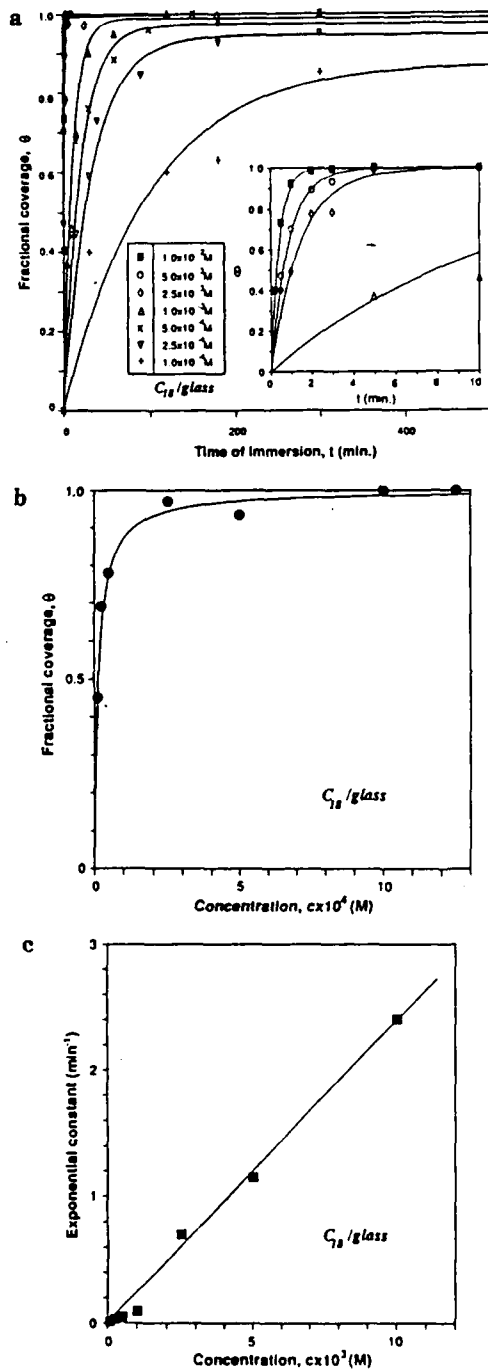
FNN28
FNP81

Figure 5. Fluorescence emission peak intensity, 377 nm, of $Py-C_{16}/C_{xx}$ mixed monolayers adsorbed on aluminum substrates from solutions of 0.005 M total acid concentration containing 1–4.8% of $Py-C_{16}$ by mole, with host fatty acid chain length between 14 and 22.

FNN28
FNP61

Figure 6. Kinetic model fitting of C_{18} adsorption on glass slides: (a) Fractional surface coverage as a function of time and solution concentration. Data points were calculated from 2920-cm^{-1} transmission IR peak intensities such as shown in Figure 3a; curves were fitted with κ values obtained from Figure 6b and an exponential time constant in eq 2. (b) Equilibrium coverage (with immersion times > 24 h) as a function of concentration; curves were fitted with eq 3, the Langmuir isotherm. (c) Check of fitting of eq 2 by the correlation of the exponential constant and concentration, c.

CAP00 1
CAP03 10
     21
     28
Figure 7. Kinetic model fitting of C_{18} adsorption on aluminum substrates: (a) fractional coverage as a function of time and solution concentration; (b) equilibrium coverage (with immersion times > 24 h); for details see Figure 6.

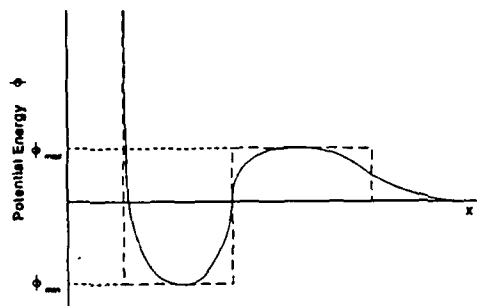(c) Check of fitting;

CAP00   1   **Figure 8.** Typical one-dimensional interaction energy profile near
CAP03   8   a surface.
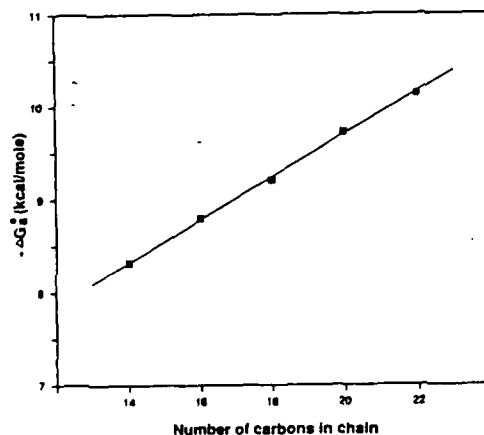

CAP00   1   **Figure 9.** Free energy of adsorption of fatty acids on aluminum
CAP03   11 at infinite dilution as a function of carbon chain length, calculated
        22 from data shown in Figure 7 and eq 5.

TTL20

Table I. Film Thickness of Alkanoic Acids Adsorbed from Solutions in HD on (Oxidized) Aluminum Substrate from Ellipsometric Measurements[a]

HDB40

adsorbate	myristic acid	palmitic acid	stearic acid	arachidic acid	behenic acid
ROW50 no. of carbons	14	16	18	20	22
ROW60 extended molecular length (Å)	19.4	21.9	24.5	27.0	29.5
ROW70 film thickness (Å)	19.5 ± 1.5	21.0 ± 1.5	23.6 ± 2	27.3 ± 2	29.6 ± 2

FNT80 [a] Solution concentration 0.01 M (C_{14}, C_{16}, C_{18}) and 0.005 M (C_{20}, C_{22}); immersion time 30 min.

AID00 INITIAL TABLE WIDTH IS DOUBLE COLUMN

TTL20 Table II. Order of Magnitude Comparison of the Adsorption Rate Constants Measured in Different Systems

HDB40

substance	adsorption system	κ, mol/cm^3	k_a/N_0, cm^3/(mol·s)	k_d/N_0, s^{-1}	ref
ROW50 n-alkane sulfonates (C_{10}–C_{14})	water → alumina particles	3×10^{-8}–1×10^{-6}	4×10^4–7×10^4	7×10^{-3}–9×10^{-2}	21
ROW60 sulfonate (C_{14})	water → glass particles	6×10^{-7}	2×10^4	1×10^{-2}	21
ROW70 n-alkyl benzenesulfonates (C_{10}–C_{12})	water → Berea sandstone particles	8×10^{-8}–1×10^{-7}	2×10^2–6×10^2	2×10^8–6×10^{-5}	22
ROW80 dodecyl benzenesulfonate (C_{12})	water → alumina particles	3×10^{-6}	1×10^3	4×10^{-3}	23
ROW90 n-alkyltrimethylammonium bromdies (C_{10}, C_{16})	water → alumina particles	8×10^{-8}–7×10^{-7}	4×10^4–6×10^4	8×10^{-3}–3×10^{-2}	21
ROW100 cetyltrimethylammonium bromide (C_{16})	water → glass particles	8×10^{-8}–3×10^{-8}	1×10^4	2×10^{-2}	21
ROW110 oxyethylenated nonylphenols (C_9–C_{30})	water → Berea sandstone particles	5×10^{-8}–1×10^{-7}	2×10^2–6×10^2	1×10^{-6}–8×10^{-6}	22
ROW120 cetylpyridinium chloride (C_{16})	water → TiO$_2$ particles	4×10^{-8}	6×10^2	2×10^{-1}	23
ROW130 Aerosol-OT (C_8)	water → Ge plate		1×10^2		15
ROW140 Aerosol-OT (C_8)	heptane → Ge plate		2×10^2		15
ROW150 stearic acid (C_{18})	hexadecane → glass plate	1.5×10^{-8}	1.2×10^3	1.8×10^{-6}	this work
ROW160 stearic acid (C_{18})	hexadecane → Al plate	5×10^{-10}	4×10^6	2×10^{-4}	this work

[handwritten annotations: "— bromides", "tetradecane ∩ sulfonate ±", "will be ok on final", "—b"]

AID00 INITIAL TABLE WIDTH IS DOUBLE COLUMN

TTL20 Table III. Comparison of the Contribution of the Free Energy of Adsorption per Unit Hydrocarbon Chain Length of Surfactant Measured in Different Systems

HDB40

substance	adsorption system	W cal/mol	ref
ROW50 n-alkanoic acids	oil → oil/Pt interface	1200	24
ROW60 n-alkylamines	oil → oil/Pt interface	400	24
ROW70 n-alkanoic acids	oil → oil/Al interface	230	this work
ROW80 n-alkyl alcohols	melt → melt/Pt interface	188	24
ROW90 n-alkanoic acids	melt → melt/Pt interface	212	24
ROW100 n-alkylamines	melt → melt/Pt interface	336	24
ROW110 n-alkanamides	melt → melt/Pt interface	103	24
ROW120 n-alkanoic acids	water → oil/water interface	830	25
ROW130 n-alkyl alcohols	water → air/water interface	750	26
ROW140 n-alkanoic acids	water → air/water interface	690	26
ROW150 n-alkanoic acids	water → air/water interface	770	27
ROW160 n-alkyl alcohols	vapor → Hg/air interface	570	26

AID00 INITIAL TABLE WIDTH IS SINGLE COLUMN

The number of words in this manuscript is 6313.

The manuscript type is A.

Running Heads

Self-Assembled n-Alkanoic Acid Monolayers

Chen and Frank

Author Index Entries

Chen, S. H.

Frank, C. W.

Text Page Size Estimate = 5.4 Pages

Graphic Page Size Estimate = 3.4 Pages

Total Page Size Estimate = 8.7 Pages